



PCCP

**Importance of self-interaction-error removal in density functional calculations on water cluster anions**

Journal:	<i>Physical Chemistry Chemical Physics</i>
Manuscript ID	CP-ART-11-2019-006106.R1
Article Type:	Paper
Date Submitted by the Author:	14-Dec-2019
Complete List of Authors:	Vargas Tellez, Jorge; University of Texas at El Paso, Physics Ufondu, Peter; University of Texas at El Paso, Physics Baruah, Tunna; University of Texas at El Paso, Physics Yamamoto, Yoh; University of Texas at El Paso Jackson, Koblar; Central Michigan University, Physics Zope, Rajendra; University of Texas at El Paso, Physics

SCHOLARONE™  
Manuscripts

# Importance of self-interaction-error removal in density functional calculations on water cluster anions

Jorge Vargas,<sup>a†</sup> Peter Ufondu,<sup>†</sup> Tunna Baruah,<sup>†,¶</sup> Yoh Yamamoto,<sup>†</sup> Koblar A.  
Jackson,<sup>‡</sup> and Rajendra R. Zope<sup>\*,†,¶</sup>

<sup>†</sup>*Department of Physics, The University of Texas at El Paso, El Paso, Texas, 79968*

<sup>‡</sup>*Physics Department and Science of Advanced Materials Program, Central Michigan  
University, Mt. Pleasant Michigan, 48859*

<sup>¶</sup>*Computational Science Program, The University of Texas at El Paso, El Paso, Texas,  
79968*

E-mail: rzope@utep.edu

---

<sup>a</sup>Current address: Unidad Academica de Fisica, Universidad Autonoma de Zacatecas, Calz. Solidaridad  
Esq. Paseo de la Bufa S N, Zacatecas, Mexico. C.P. 98060

## Abstract

Accurate description of the excess charge in water cluster anions is challenging for standard semi-local and (global) hybrid density functional approximations (DFAs). Using the recent unitary invariant implementation of the Perdew-Zunger self-interaction correction (SIC) method using Fermi-Löwdin orbitals, we assess the effect of self-interaction error on the vertical detachment energies of water clusters anions with the local spin density approximation (LSDA), Perdew-Burke-Ernzerhof (PBE) generalized gradient approximation, and the strongly constrained and appropriately normed (SCAN) meta-GGA functionals. Our results show that for the relative energies of isomers with respect to reference CCSD(T) values, the uncorrected SCAN functional has the smallest deviation of 21 meV, better than that for the MP2 method. The performance of SIC-SCAN is comparable to that of MP2 and is better than SIC-LSDA and SIC-PBE, but it reverses the ordering of the two lowest isomers for water hexamer anions. Removing self interaction error (SIE) corrects the tendency of LSDA, PBE, and SCAN to over-bind the extra electron. The vertical detachment energies (VDEs) of water cluster anions, obtained from the total energy differences of corresponding anion and neutral clusters, are significantly improved by removing self-interaction and are better than the hybrid B3LYP functional, but fall short of MP2 accuracy. Removing SIE results in substantial improvement in the position of the eigenvalue of the extra electron. The negative of the highest occupied eigenvalue after SIC provides an excellent approximation to the VDE, especially for SIC-PBE where the mean absolute error with respect to CCSD(T) is only 17 meV, the best among all approximations compared in this work.

## Introduction

The hydrated electron is a system that has long attracted the attention of the scientific community<sup>1-6</sup> due to its importance in chemical and biological processes, such as atmospheric chemistry<sup>7</sup> or radiation damage in DNA,<sup>8</sup> to name just two. In this context, systematic

study of water cluster anions can be useful for obtaining insights into the behavior and evolution of electron hydration. Indeed, since the first observation of a free hydrated electron in the gas phase<sup>9</sup>, a large number of studies have been performed on water cluster anions resulting in debate about whether the extra electron is bound in a delocalized surface state or bound internally in a cavity.<sup>10–15</sup> Even before its first observation, theoretical models for the hydrated electron were proposed<sup>16,17</sup>. Later, improvements in experimental techniques allowed direct comparison with theoretical results. Photoelectron spectroscopy<sup>18–24</sup> and vibrational spectroscopy<sup>25–29</sup> techniques have been used to garner information about the structural and electronic properties of water cluster anions. These experiments have provided data for the vertical detachment energy (VDE) of small water clusters. The VDE is the energy required to remove an excess electron from an anion. Moreover, a combination of simulations and experimental vibrational spectra has been used to identify the structure of stable isomers<sup>26,30,31</sup>. It is, however, in general difficult to assign a particular isomer to the observed experimental spectra as the experiments usually sample non-equilibrium ensembles of clusters. A detailed description of the challenges involved in ascribing specific spectroscopic features to an individual isomer of  $(\text{H}_2\text{O})_6^-$  is provided by Choi and Jordan in Ref. 32.

Accurate description of a hydrated electron poses a significant challenge to density functional approximations (DFAs). In general, DFAs are inadequate for describing the binding of the excess electron. As a result, most computational studies on small anionic water clusters<sup>10,19,30,33–43</sup> have used a post Hartree-Fock (HF) method like the Møller-Plesset perturbation method (MP2) or the coupled cluster method with single, double and perturbative triple excitations CCSD(T). CCSD(T) is computationally very demanding and has only been used to study small clusters and often in these studies, structural relaxation is carried out by a faster method like MP2.

Many failures of the DFAs have been ascribed to the self-interaction error (SIE) present in the approximate exchange-correlation functionals. The SIE occurs due to the incomplete

cancellation of the self-Coulomb by the approximate self-exchange energy. This error is particularly dominant in the local and semi-local approximations and is mitigated to some extent in the hybrid DFAs due to the addition of HF exchange. It has, however, been found that the most popular global hybrid functional B3LYP<sup>44</sup> significantly overestimates the VDEs of anionic water clusters. On the other hand, a recently proposed non-empirical meta-GGA functional (SCAN)<sup>45</sup> has been found to provide an excellent description of the structural, electronic, and dynamic properties of liquid water<sup>46</sup>. The SCAN meta-GGA functional, unlike most other DFAs, also predicts the energetics of gas-phase water hexamers and ice phases with quantitative accuracy<sup>45</sup>.

In this work we examine the role of SIE in three non-empirical functionals that belong to the lowest three rungs of Jacob’s ladder on the VDEs of water. The functionals used here are the local density approximation (LDA), generalized gradient approximation (GGA) given by Perdew, Burke, Ernzerhof (PBE)<sup>47</sup>, and the SCAN meta-GGA functional<sup>45</sup>. The incorrect asymptotic form of the DFA potential caused by SIE is expected to have a particularly strong impact on the description of anionic systems which typically have a weakly bound extra electron in a diffuse orbital. We explicitly remove SIE using the self-interaction correction (SIC) applied to the DFA’s. We study both the effect of SIC on the orbital energy of the highest occupied electron orbital and on the total energy difference between corresponding anion and neutral systems. We also check the error made by using the SCAN functional for calculating the VDE. The details of the self-interaction correction method and the computation scheme is presented in the next section followed by the results and discussion.

## Methodology

In 1981, Perdew and Zunger proposed an orbital-wise correction to remove the self-interaction error<sup>48</sup> in density functional approximations. In the Perdew-Zunger self-interaction correc-

tion (PZSIC) method the exchange-correlation energy is corrected as

$$E_{\text{XC}}^{\text{SIC}}[\rho_{\uparrow}, \rho_{\downarrow}] = - \sum_{i, \sigma}^{N_{\sigma}} \{U[\rho_{i\sigma}] + E_{\text{XC}}[\rho_{i\sigma}, 0]\}, \quad (1)$$

where  $i$  runs over the  $N_{\sigma}$  occupied orbitals of spin  $\sigma$ , and  $\rho_{i\sigma}$  is the  $i^{\text{th}}$  orbital density. The terms  $U[\rho_{i\sigma}]$  and  $E_{\text{XC}}[\rho_{i\sigma}, 0]$  are the exact self-Coulomb and approximate self exchange correlation (XC) energies, respectively. The correction vanishes when  $E_{\text{XC}}$  is the exact XC functional. Pederson et al. have shown that the orbitals minimizing the PZ-SIC total energy must satisfy the conditions known as the localization equations:<sup>49,50</sup>

$$\langle \phi_{j\sigma} | V_{j\sigma}^{\text{SIC}} - V_{i\sigma}^{\text{SIC}} | \phi_{i\sigma} \rangle, \quad (2)$$

where  $V_{i\sigma}^{\text{SIC}}$  is the SIC potential for the  $i^{\text{th}}$  orbital. Satisfying the localization equations is a computationally slow process and the self-interaction corrected energy obtained as a result is not guaranteed to be size-consistent.

A recent scheme for SIC proposed by Pederson, Ruszinzsky and Perdew<sup>51</sup> circumvents the need for satisfying Eq. [2]. The localized orthonormal set of orbitals is derived from Fermi orbitals which depend on the density matrix and the spin density as:

$$\phi_{i\sigma}^{\text{FO}}(\mathbf{r}) = \frac{\sum_j \psi_{j\sigma}^*(\mathbf{a}_{i\sigma}) \psi_{j\sigma}(\mathbf{r})}{\sqrt{\sum_j |\psi_{j\sigma}(\mathbf{a}_{i\sigma})|^2}} = \frac{\gamma_{\sigma}(\mathbf{a}_{i\sigma}, \mathbf{r})}{\sqrt{\rho_{\sigma}(\mathbf{a}_{i\sigma})}}, \quad (3)$$

where  $\gamma_{\sigma}(\mathbf{a}_{i\sigma}, \mathbf{r})$  is the single-particle density matrix of the KS system, and  $\mathbf{a}_{i\sigma}$  are a set of points in real space called the Fermi orbital descriptors (FODs). The Fermi orbitals are normalized, but are not orthogonal. They are orthogonalized using Löwdin's method of symmetric orthonormalization<sup>52</sup> resulting in an orthonormal set of local orbitals called Fermi-Löwdin orbitals (FLOs). The positions of the FODs determine the Fermi orbitals and different choices lead to different total energies. The optimal positions of the FODs are obtained in a procedure that is analogous to a molecular geometry optimization. The

gradients of the energy with respect to the FODs can be calculated<sup>53,54</sup> and used in a preconditioned limited-memory Broyden, Goldfarb, Shanno (LBFGS) algorithm<sup>55</sup>. The FODs are updated after each self-consistent FLOSIC calculation. The optimization is carried out until the forces on all FODs drop below 0.0001 Ha/Bohr.

The Fermi-Löwdin orbital based self-interaction correction (FLO-SIC) method is implemented in the FLOSIC code<sup>56,57</sup> that is based on the UTEP-NRLMOL code<sup>58,59</sup>. This code uses a Gaussian basis set<sup>60</sup>, and a variational integration mesh<sup>61</sup> to perform numerically precise calculations on molecules composed of non-relativistic atoms. The FLOSIC implementation has been used to study a number of different properties for systems ranging in size from atoms<sup>62,63</sup> and small molecules to larger molecules such as Mg-porphyrin and C<sub>60</sub><sup>64</sup>. FLOSIC has been used to study various properties ranging from energetic properties such as atomization energies<sup>56</sup>, barrier heights<sup>56,65,66</sup>, magnetic properties<sup>67,68</sup> to density dependent properties such as dipole moment<sup>69</sup> and polarizability<sup>70</sup>.

We use the default Pederson-Porezag NRLMOL basis<sup>60</sup> that is specially optimized for the Perdew-Burke-Ernzerhof (PBE)<sup>47</sup> generalized gradient approximation (GGA). The calculations are spin-polarized for systems with net spin. To obtain an accurate description of water anions, extra diffuse functions are added to account for the more diffuse charge distribution in these systems<sup>39</sup>. We used the same exponents as used by Yagi *et al.*<sup>41</sup>. We have verified that these exponents give converged results for the VDEs. The exponents are  $9.87 \times 10^{-3}$  au,  $8.57 \times 10^{-3}$  au, and  $3.72 \times 10^{-3}$  au for oxygen *s*, *p*, and hydrogen *s* respectively.

Yagi and coworkers reported the anionic water cluster geometries optimized at the MP2 level which they used subsequently to perform the CCSD(T) calculations<sup>41</sup>. To facilitate a direct comparison with the earlier MP2 and CCSD(T) results, we used the same set of MP2 optimized geometries from Ref. 41 in our calculations.

Each water molecule has five electrons of each spin. The FODs representing the valence electrons of each molecule form a tetrahedral structure with the center at the oxygen atom and two of the vertices along the two O-H bonds. The tetrahedral structure can be seen

in Fig. 1. The FOD representing the oxygen core orbital is found to be at the oxygen nuclear position. The extra FOD for the anions is initially placed at the central region of the singly occupied molecular orbital obtained at the PBE level. The position of this FOD is then optimized along with all the others using the pre-conditioned LBFGS routine outlined above.

The VDE can be calculated as the total energy difference between the energy of the anion and neutral cluster at the geometry of the anion. The negative of the energy of the highest occupied molecular orbital (HOMO) also mimics the negative of the electron removal or detachment energy<sup>71-74</sup>. The HOMO eigenvalue for an anion in a DFA calculation is generally found to be positive, corresponding to an unbound outer electron. Therefore the detachment energies can only be calculated from total energy differences when using DFAs. As shown below, the anion HOMO in FLOSIC-DFA calculations is negative and a good approximation to the removal energy. We examine the VDEs calculated from total energies as well as from the HOMO eigenvalues for the FLOSIC calculations.

## Results and discussion

The anionic water clusters contain a weakly bound extra electron. The 20 water isomers  $(\text{H}_2\text{O})_n^-$  in the range  $n = 2 - 6$  studied here can be grouped by various types of extra electron binding motifs. The clusters studied here and other slightly different clusters have been reported in several studies with different names<sup>10,19,34,37,42</sup>. For direct comparison with the work of Yagi and coworkers<sup>41</sup>, we follow their naming conventions. The anionic water clusters are classified as linear(L), double acceptor (AA), donor(D), and internal (I). In linear (L) clusters the water molecules are bound by successive hydrogen bonds (HB). These structures tend to have the smallest number of HBs among all the isomers. The AA type clusters have one double-acceptor water molecule such that its hydrogen atoms are not involved in any HB. In the D type clusters the extra electron is bound collectively by dangling O-H

bonds. In I type anions the extra electron is trapped internally, as in a cavity.

The water clusters studied here are presented in figures 1–5, where the positive electron density difference (EDD) between the anionic and the neutral systems shows the charge density of the extra electron. The density difference also contains rearrangements of the neutral molecule density due to the presence of the extra electron, but such differences are insignificant compared to density of the extra electron itself. The FLOSIC calculations of the water anions were started with the same FOD positions as for the neutral water cluster but with one extra FOD. All the FODs are fully re-optimized for the anionic clusters. For simplicity, only the optimized extra FOD position is shown in Figs 2-5 and an image including all the FODs is shown for the anionic water dimer in Fig. 1.

The number and strength of the HBs in a cluster determine its stability<sup>41</sup>. For most of the water cluster sizes studied here, the isomers with dangling O-H bonds (D) are the lowest energy structures. The D structures are cyclic, with every water molecule being both donor and acceptor of a hydrogen bond and the dangling O-H bonds oriented toward the same direction where most of the extra charge is accommodated<sup>41</sup>. Moreover, it was shown that the orientations of the dangling O-H bonds in most stable anionic clusters are different from those for the neutral clusters<sup>41</sup>. In neutral water clusters of size up to  $n=5$ , the most stable isomers have the dangling OH bonds on alternating sides of a quasi-planar polygon<sup>35,37</sup>.

In the neutral water dimer, the torsional angle between the bisecting axis of the proton acceptor and the line segment connecting the oxygens is experimentally found to be  $57^\circ$ <sup>75</sup>. Kim et al. studied several configurations of the water dimer<sup>35</sup> at the CCSD(T) level. They concluded that the presence of the extra electron in the dimer introduces a large change in the torsional angle. They also concluded that the anionic water dimer is a very floppy structure with large vibrational zero-point energy effects. Among the reported structures of the neutral water dimers, the *trans* isomer has a dipole moment of 2.7D whereas nearly isoenergetic *cis* isomer has a dipole moment of 4.3D. The individual dipoles of the water molecules are almost parallel in the *cis* configuration. Thus, although the total energies of

**Table 1: Relative energies in meV of the different water cluster anions with respect to the D isomers. The dipole moment in Debye,  $\mu$ , is from the SIC-SCAN calculations of the neutral clusters. The mean absolute deviation (MAD) is with respect to the CCSD(T) values.**

Cluster	CCSD(T) <sup>a</sup>	MP2 <sup>a</sup>	B3LYP <sup>a</sup>	DFA			FLOSIC			$\mu$
				LDA	PBE	SCAN	LDA	PBE	SCAN	
3D	–	–	–	–	–	–	–	–	–	4.03
3L	69	78	9	99	45	92	145	111	111	7.13
3AA	147	173	87	282	131	169	248	156	177	6.40
3I-2	178	204	113	304	144	185	271	174	197	6.39
3I-1	533	551	343	784	407	512	714	461	503	1.75
4D	–	–	–	–	–	–	–	–	–	5.17
4AA	134	178	121	329	185	180	282	208	180	8.92
4L	191	208	134	375	194	224	317	215	199	9.39
4I	425	451	308	706	375	429	656	469	471	0.00
5D	–	–	–	–	–	–	–	–	–	5.39
5AA-2	-30	30	43	67	84	-23	104	149	-7	9.03
5AA-1	139	186	134	305	177	165	294	217	88	9.48
5L	204	225	147	422	228	242	357	241	225	10.77
5I	152	208	139	268	157	127	310	268	165	8.71
6D	–	–	–	–	–	–	–	–	–	5.51
6AA-2	-56	-13	-9	21	16	-51	70	94	13	10.41
6AA-1	117	182	126	248	151	106	317	291	210	10.24
6L	351	356	252	633	327	387	544	345	377	13.09
6I	516	533	382	906	446	524	864	596	619	0.00
MAD	–	32	66	383	204	21	168	73	39	0.30

<sup>a</sup> Ref. 41

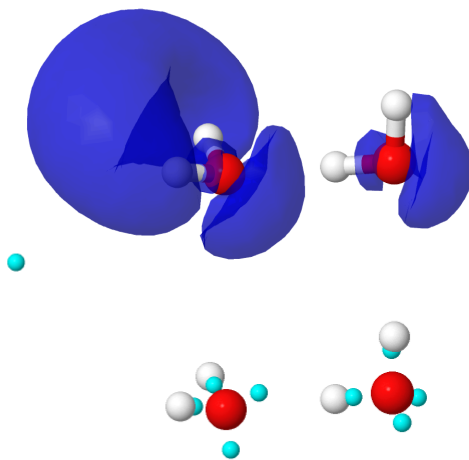


**Figure 1: (Top)** Electron density difference (blue) of anionic water dimer anion and **(bottom)** the optimized FODs shown as cyan spheres.

the two anions are very close, it was shown<sup>35</sup> that the *trans* isomer barely binds an extra electron, while the *cis* isomer has significantly more binding due to its larger dipole. Based on these earlier reports, FLOSIC calculations were performed on the *cis* isomer. In Fig. 1 the EDD of the *cis* isomer (2L) and the positions of the FODs are shown. As mentioned above, the FODs corresponding to the valence electrons form a tetrahedron around each oxygen atom and the extra FOD for the anion finds its optimal place at the  $\angle$ H-O-H bisector, but far away (4.4 Å) from the acceptor molecule. The figure shows the location of the extra electron density in the anion which is in the same direction as the extra FOD. A similar pattern is observed in all the other clusters. For that reason, only the extra FOD is shown in figures 2–5, together with the EDD.

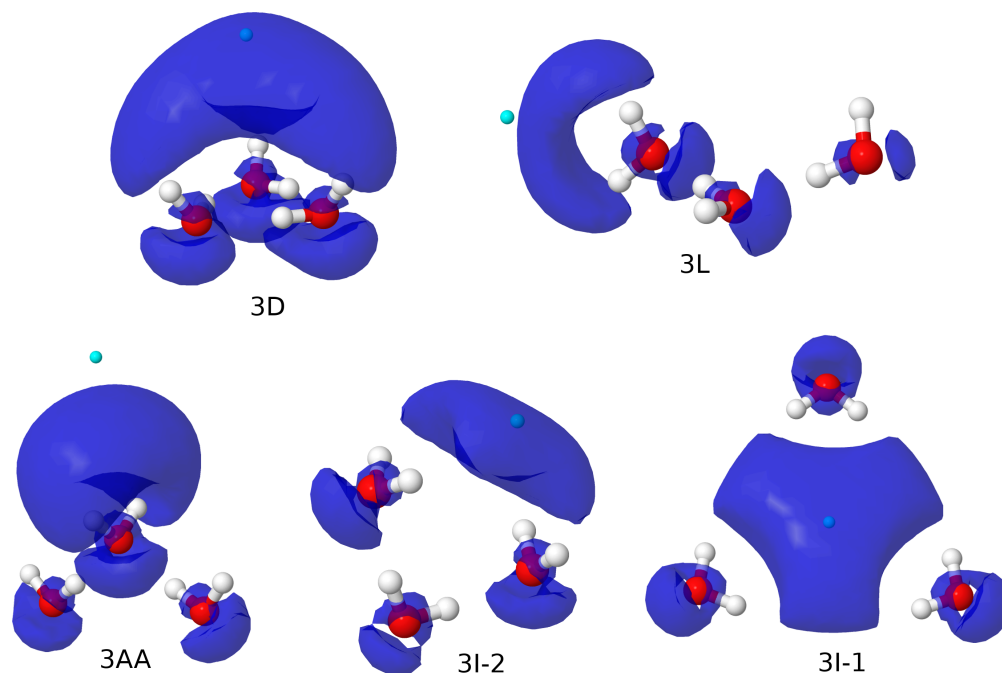


Figure 2: Water trimer anions with the EDD in blue and the optimized extra FOD of each isomer.

The EDD plots of the various trimer, tetramer, pentamer and hexamer isomers are shown in Fig. 2 - 5. The plots corresponding to various functionals are similar and therefore we show only the FLOSIC-LDA version. The FLOSIC EDD plots are in close agreement with the plots shown in Ref.<sup>41</sup>. The D structures show a collective cloud of the extra electron

spread over multiple water molecules. From the trimer to the pentamer, the D structures have the water monomers forming a quasi-planar structure, but in case of the hexamers, the monomers in the D structure form a 3-dimensional book structure. However, for all sizes, the excess electron cloud is spread over the whole structure. In all the linear isomers, there is one only-donor and one only-acceptor water molecule with the intermediate molecules being both a donor and an acceptor of a HB. The excess charge of the anion is mainly accommodated in front of the dangling hydrogen atoms of the only-acceptor molecule. On the other hand, the double acceptor isomers have one molecule which attracts the excess electron cloud. In the case of the hexamers, two such double acceptor structures were examined. In the 6AA-1 isomer, there are two water molecules that are both double-acceptors. These two molecules contribute equally to accommodate the extra charge in 6AA-1, whereas in the 6AA-2 isomer the extra electron is mainly located around the only double acceptor water molecule. The I structures with internally trapped electrons are found to be higher in energy for the sizes under study here. The 3I-1 has  $D_{3h}$  symmetry and the 4I structure has a center of inversion and, therefore, both have zero net dipole. Both 3I-2 and 5I structures have two water molecules that form a "bridge" for the extra charge.

The EDD plots mainly show the extra electron density as a diffuse cloud. We find that the extra FOD in the anionic cluster generally follows the cloud and is located away from the molecular framework. Our calculations also show that the dipole of the neutral cluster plays a minor role in the binding of the extra charge. As seen from Table 1, the dipole moment of the lower-energy clusters are in fact smaller than those of many high-lying isomers. In general, the linear (L) structure, which has a chain of HBs, has a larger dipole moment compared to the ring-like D structure.

The relative energies of the anionic water clusters with  $n=3-6$  are presented in Table 1. For the sizes  $n=3$  and 4, the relative energies follow similar trends across all methods used here, including the FLOSIC-DFAs. The D structures of the trimer and tetramer are found to be the lowest energy isomer by all the methods (Cf. Table 1). The D structures are ring-like

for both sizes. For the trimers, all the computational methods also put the linear isomer (3L) as the second lowest isomer. However, Hammer et al.<sup>30</sup> identified the linear structure for the trimer anion from infrared spectrum and theoretical calculations on the vibrational spectra of the trimer anion. Similarly, the 4AA isomer has been experimentally identified for the tetramer.<sup>21</sup> Shin et al. also found weaker signals in their photo-electron spectra that can be ascribed to 4L and 4D, but the major presence of the 4AA isomer was unequivocally confirmed through IR experiments and B3LYP vibrational spectra comparisons<sup>10</sup>. The 5D isomer, which is presumably optimized from the  $C_5$  ring with the five oxygen atoms forming a planar pentagon, does not conform to a planar structure upon optimization. One water molecule moves out-of-plane, while the two adjacent molecules reorient their dangling hydrogen atoms radially outward thus diminishing the characteristic collective cloud of the D isomers. From the pentamer onward, the D structure is not the lowest energy isomer at the CCSD(T) level. The same ordering is also seen with the SCAN functional.

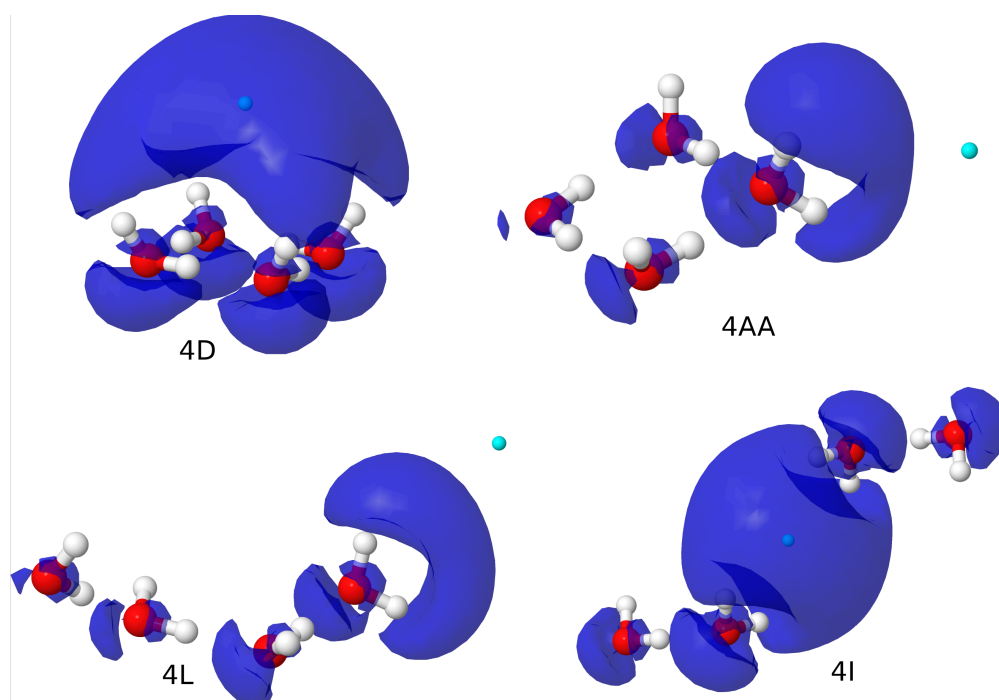


Figure 3: Water tetramer anions with the EDD in blue and the optimized extra FOD of each isomer.

Since the first experiments on the water clusters, the hexamer was identified as a magic

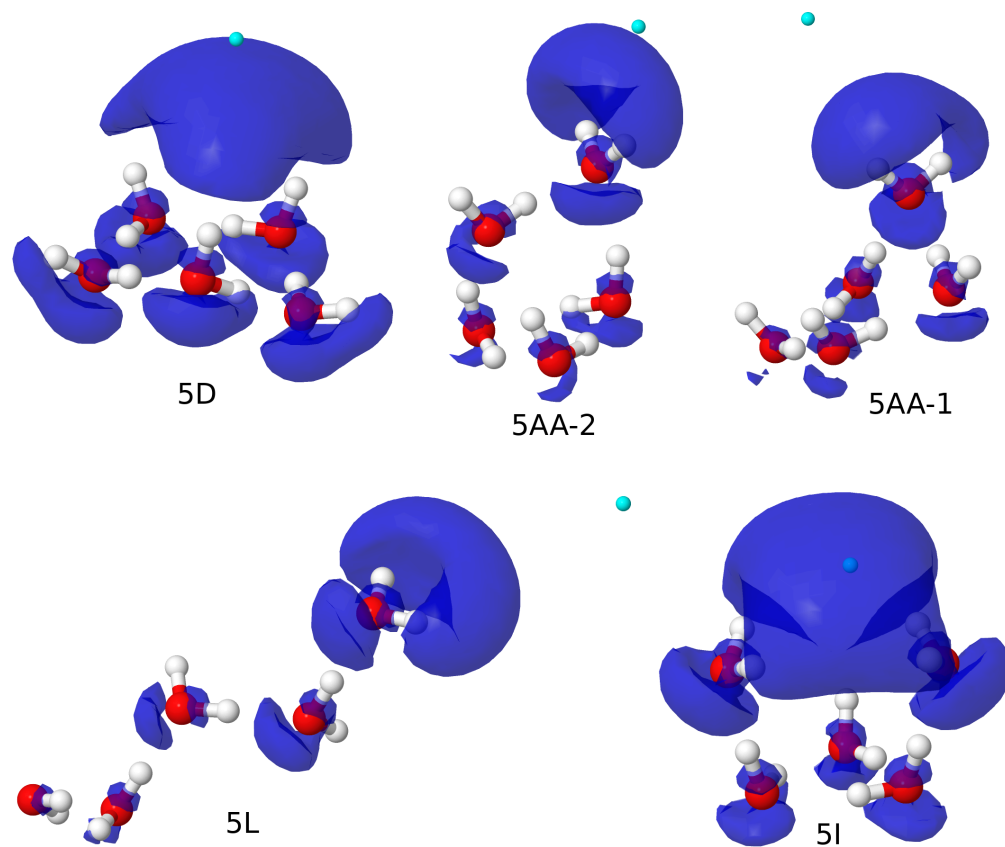


Figure 4: Water pentamer anions with the EDD in blue and the optimized extra FOD of each isomer.

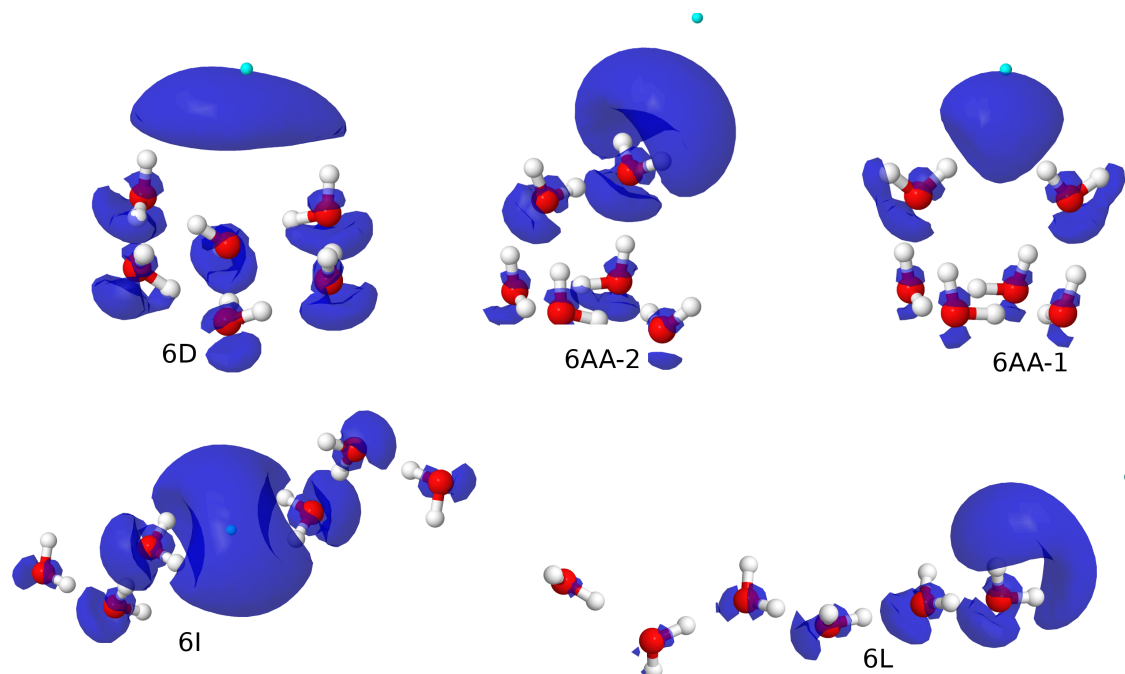


Figure 5: Water hexamer anions with the EDD in blue and the optimized extra FOD of each isomer.

number for the water cluster anions<sup>9,18</sup> and has been extensively studied. It is broadly accepted that the experimental signal comes mainly from the 6AA-2 isomer with some contribution of the 6D<sup>25,31,37</sup>. The CCSD(T) as well as MP2 and B3LYP calculations from Ref.<sup>41</sup> predict the 6AA-2 structure as the lowest energy isomer. The SCAN meta-GGA functional makes the same prediction. On the other hand, the FLOSIC method with all three different functionals predicts the 6D isomer to be the lowest energy structure. The 6D is the so-called book structure and the collective cloud is more concentrated on the two upper molecules as depicted in Fig. 5. The 6AA-2 can be thought of as a combination of the 4D isomer and the water dimer. The 6AA-1 and 6AA-2 structures are related to the so-called prism structure, which is one of the most stable neutral hexamers. The difference is that in the structure of the anions, the prism has one broken edge. In the 6AA-1 isomer there are two double acceptor molecules without any HB between them. These two molecules contribute equally to accommodate the extra charge in 6AA-1, whereas in the 6AA-2 isomer the extra electron is mainly located around the single double acceptor water molecule. 6AA-2 is favored over

6AA-1 by CCSD(T), MP2, B3LYP, and the SCAN functional. The relative energies of these double acceptor clusters are comparable in SCAN and CCSD(T). The 6L and 6I isomers, with the largest and smallest dipole moments, respectively, have significantly higher energies in all methods and are not likely to be found experimentally. Although the isomer ordering of the hexamers using SCAN agrees with that of CCSD(T), the SIC-SCAN results show same ordering as for SIC-LSDA and SIC-PBE.

Overall, the SCAN meta-GGA functional results for the stability of the anionic clusters are in close agreement with the CCSD(T) predictions. The ordering of all the isomers is the same and the mean absolute deviation (MAD) of relative energies is only 21 meV. The energy ordering of isomers for the smaller anionic clusters containing 3 and 4 water molecules is the same for all three functionals and their FLOSIC counterparts. For  $n=5$  and 6, LDA and PBE and FLOSIC-LDA and FLOSIC-PBE all invert the ordering of the two lowest-energy isomers. Both SCAN and FLOSIC-SCAN give the correct order for these isomers for  $n = 5$ , but only SCAN does for  $n = 6$ . We also find that the deviation of the relative energies from the CCSD(T) values is reduced significantly upon removal of self-interaction error from LDA and PBE. For LDA, the MAD decreases from 383 meV to 168 meV, and for PBE, from 204 meV to 73 meV. On the other hand, correcting for self-interaction in SCAN increases the MAD from 21 meV to 39 meV. The performance of the SCAN functional is the best among all approximations including MP2. This observation is consistent with earlier results where the SCAN functional was found to provide an excellent description of the ordering<sup>45,76</sup> of the neutral water hexamers, as well as the ordering of various phases of ice. It should be noted that SCAN is a meta-GGA functional whose correlation component is already self-interaction free. Removal of SIE from SCAN results in over-correcting, resulting in a somewhat degraded performance. However, FLOSIC-SCAN results are still comparable to MP2.

## Vertical detachment energies

The VDEs calculated from total energy differences between neutral and anionic clusters with and without FLOSIC are presented in Table 2. Accurate description of the VDE is a challenge for the density functional approximations due to the inherent self-interaction present in these DFAs. Presence of SIE, in general, results in excessive electron delocalization causing significant errors in the electron binding energies. Indeed, as can be seen from the Table 2, the errors made by the pure DFAs are substantial. Since the CCSD(T) values are in excellent agreement with the available experimental values and also because the CCSD(T) values are available for all the clusters studied here, we calculate the errors in DFAs and SIC-DFAs with respect to the CCSD(T) results. The mean absolute error (MAE) in VDE with respect to CCSD(T) results are 339, 247, and 127 meV for LSDA, PBE, and SCAN, respectively. These numbers highlight the tendency of these functionals to over-bind an extra electron to water clusters, but they also show that as one climbs the Perdew-Schmidt Jacob's ladder<sup>77</sup> of increasingly complex functionals, the tendency decreases. The fourth rung of functionals corresponds to the hyper-GGA functionals. The hybrid functionals that include a certain fraction of HF exchange belong to this rung. In many situations, HF calculations have errors that are opposite to those made by DFAs. This often results in better descriptions of properties by hybrid functionals compared to standard DFAs. However, in the case of the VDE of water cluster anions, the popular global hybrid B3LYP gives no improvement. In fact, it can be seen from Table 2 that the MAE with B3LYP (238 meV) is comparable to that with PBE, which sits two rungs lower on Jacob's ladder. The performance of SCAN is substantially better than B3LYP. This may be due to the correlation component of the SCAN functional being self-interaction free. It is consistent with recent reports<sup>45,46</sup> that show SCAN provides a much improved description of liquid water and neutral water clusters than other DFAs, and with the fact that SCAN gives the correct ordering of water cluster anion isomers ordering as discussed above.

The relatively poor performance of B3LYP despite having an admixture of HF exchange

is perplexing. The over-binding tendency of B3LYP, or, in other words, the effect of mixing HF with DFAs on the electronic properties, was investigated by Yagi and coworkers<sup>41</sup>. These authors studied water cluster anions using the long-range corrected DFAs (LC-DFAs). In this approximation, the electron repulsion operator is divided into short-range and long range parts with the short range part being described by the DFA and the long-range orbital-orbital exchange interaction described using HF exchange. They used the BLYP<sup>78,79</sup> and BOP<sup>78,80</sup> functionals for the short-range. Their results showed that both the LC-BLYP and LC-BOP functionals provided significant improvement in predicting VDEs over the global hybrid B3LYP. They attributed the excellent performance of the LC-BOP functional (MAE 35 meV) over the LC-BLYP functional (MAE 152 meV) to the satisfaction of fundamental conditions by the BOP functional and violation of them by BLYP. Their results show that good estimates of VDE comparable to those of MP2 can be obtained using long range corrected functionals.

It is interesting to compare the performance of these range-corrected functionals with the present approach where the self-interaction is explicitly removed on an orbital by orbital basis using the Perdew-Zunger method. We find that the removal of self-interaction error significantly improves the VDE obtained from the total energy differences of anion and neutral clusters. The VDEs obtained from the total energy differences for the SIC-LSDA, SIC-PBE, and SIC-SCAN functionals are summarized in Table 2. The MAE in VDEs for the three SIC-DFAs are 180 meV for SIC-LSDA, 60 for SIC-PBE, and 57 meV for SIC-SCAN. These errors can be compared to those for the uncorrected functionals - 339 meV for LSDA, 247 meV for PBE, and 127 for the SCAN. This indicates that the SIE is a large contributor to the over-binding tendency of these approximations.

To better understand the nature of these errors, we used the self-interaction corrected densities obtained in the SIC-DFA calculations to evaluate the uncorrected DFAs. We then used these to recompute the VDEs. Following the notation adopted in the literature, this approach is called DFA@SIC-DFA<sup>81</sup>. Using this scheme, (Cf. Table 3) we find that the MAE

in LSDA@SIC-LSDA, PBE@SIC-PBE, and SCAN@SIC-SCAN to be 303, 217, and 110 meV, respectively. This is only a slight ( $< 15\%$ ) improvement over the self-consistent DFA values. The primary source of the errors in VDEs therefore is the approximate functional and not simply the density. Burke and coworkers<sup>82</sup> categorized DFT calculations as either normal or abnormal depending on whether errors stem from the approximate functional (normal) or from the approximate density (abnormal). The comparison of VDES from the DFAs, and DFAs@SIC-DFAs show that the VDE calculations are apparently normal.

One drawback of the pure DFAs (LSDA, PBE, and SCAN) discussed above is that although the total energy of the water cluster is correctly lowered with the addition of an extra electron, the eigenvalue of the extra electron is positive within these approximations. The over-binding tendency of the DFAs discussed earlier is for VDE estimates made from the total energy difference between corresponding anion and neutral clusters. In exact DFT, the highest occupied eigenvalue equals the negative of the ionization potential<sup>71-74</sup>. This relationship does not strictly hold for approximate density functionals and in most DFAs, the absolute value of the HOMO eigenvalue substantially underestimates the first ionization potential due to self-interaction error. The positive eigenvalue of the extra electron in the water anions in DFT indicates that the extra electron is not actually bound in the complete basis set limit. The positive eigenvalue is a result of self-interaction error which makes the asymptotic potential seen by the electron positive. Removing self-interaction improves the asymptotic description of the potential and results in negative (bound) eigenvalues for the extra electron in all three SIC-DFAs used in this work. The improved description of the binding of the extra electron due to self-interaction correction can be seen from Table 2 which presents predictions of the VDE from the eigenvalues of the extra electron in the SIC-DFA calculations ( $VDE = -\epsilon_{HOMO}$ ). The eigenvalues are excellent approximations to the VDEs, especially for SIC-PBE, for which the MAE with respect to CCSD(T) estimates is only 17 meV. The MAE for SIC-SCAN and SIC-LSDA eigenvalues are 44 and 117 meV, respectively. It is not obvious why the SIC-PBE eigenvalues approximate CCSD(T) VDE better than

SIC-SCAN or SIC-LSDA. The SIC-SCAN HOMO eigenvalues agree better with the available experimental VDE values, with a MUE of 29 meV compared to 35 meV for SIC-PBE. The SIC-LDA eigenvalues have a MUE of 70 meV when compared with the experimental values. For all three functionals, the SIC-DFA HOMO eigenvalues are better approximations of the VDEs than the total energy differences. The shift of the anion eigenvalues to positions close to the removal energies underscores that the self-interaction correction is needed for a more physically correct description of water cluster anions with DFAs.

It should be noted that the positive HOMO eigenvalues in the uncorrected DFA calculations imply that the over-binding of the VDE by DFA total energy differences is actually worse than seen in Table 2. The energy of the cluster anion would be lowered by removing a fraction of the extra electron to a large distance from the cluster. The minimum energy state corresponds to removing sufficient charge to make the HOMO eigenvalue zero. Lower anion energies would give still large VDEs than those in Table 2.

## Conclusion

We have used the recently developed Fermi-Löwdin orbital self-interaction correction scheme with the LSDA, PBE, and SCAN meta-GGA functionals to study small water cluster anions. Our results show that the SCAN functional provides a very good description of isomer ordering, as well as the relative energies of isomers, when compared to CCSD(T) results. The application of FLOSIC significantly improves the agreement for SIC-LSDA and SIC-PBE relative to CCSD(T), however, the SIC-SCAN results deviate somewhat more from the reference values than SCAN. The excellent performance of SCAN for binding energies does not carry over to the description of the binding of the extra electron. The SCAN MAE (127 meV) for electron detachment energy, although smallest among the LSDA (339 meV), PBE GGA (247 meV) and also earlier reported B3LYP (238 meV) results, is still substantially larger than the MP2 MAE (44 meV). Removing self-interaction results in significantly improved

**Table 2: Vertical detachment energies and HOMO eigenvalues in meV of water cluster anions. The mean absolute deviation (MAD) is respect to the CCSD(T) values. The uncertainties of the experimental values are about  $\pm 30$  meV.**

Cluster	CCSD(T) <sup>a</sup>	MP2 <sup>a</sup>	B3LYP <sup>a</sup>	LC-BOP <sup>a</sup>	Expt	DFA-VDE			SIC-VDE			SIC-HOMO		
						LDA	PBE	SCAN	LDA	PBE	SCAN	LDA	PBE	SCAN
2L	29	9	194	28	50 <sup>b</sup>	240	205	96	121	77	63	75	30	42
3D	6	-14	184	-9		216	184	67	96	58	39	53	14	22
3L	146	115	346	161	130 <sup>b</sup>	430	373	258	288	211	203	229	148	177
3AA	187	146	399	202		489	411	300	348	245	236	276	180	216
3I-2	175	138	427	198		488	413	293	348	251	225	279	185	215
3I-1	190	155	526	227		589	502	354	438	310	233	346	205	244
4D	49	22	239	21	60 <sup>c</sup>	289	244	123	158	105	69	109	62	73
4AA	336	283	561	273	350 <sup>c</sup>	678	577	469	511	386	390	440	314	375
4L	255	214	478	283	250 <sup>c</sup>	558	483	362	407	307	313	333	236	276
4I	439	394	713	489		861	729	610	688	494	492	642	456	524
5D	61	31	285	18		329	279	146	184	130	103	129	73	89
5AA-2	376	318	592	408	410 <sup>b</sup>	732	621	511	561	418	433	484	354	415
5AA-1	370	313	600	366		738	625	510	574	437	432	501	358	407
5L	294	250	527	338		611	532	407	442	354	348	373	277	322
5I	469	406	757	516		891	754	637	730	539	587	644	467	549
6D	104	63	347	58	210 <sup>b</sup>	413	342	205	255	187	164	188	114	132
6AA-2	477	414	706	507	480 <sup>b</sup>	856	728	621	684	513	547	598	443	508
6AA-1	553	482	847	634		1026	865	746	814	600	653	737	521	616
6L	381	331	643	426		729	636	505	552	445	436	474	358	402
6I	839	793	1120	922		1349	1163	1047	1131	870	915	1145	904	1001
MAD	-	44	238	35		339	247	127	180	60	57	116	17	44

<sup>a</sup> Ref. 41, <sup>b</sup> Ref. 20, <sup>c</sup> Ref. 21

**Table 3:** VDEs (in meV) obtained using DFA total energies computed with self-consistent FLOSIC-DFA densities (DFA@FLOSIC) compared to the reported VDEs obtained with CCSD(T). The mean absolute deviation (MAD) is respect to the CCSD(T) values.

Cluster	LDA	PBE	SCAN	CCSD(T) <sup>a</sup>
2L	217	184	82	29
3D	191	165	58	6
3L	403	303	237	146
3AA	456	383	280	187
3I-2	389	389	275	175
3I-1	467	468	327	190
4D	264	223	111	49
4AA	651	545	446	336
4L	532	453	340	255
4I	844	704	584	439
5D	299	248	114	61
5AA-2	712	586	547	376
5AA-1	699	593	493	370
5L	581	496	386	294
5I	873	725	627	469
6D	380	311	190	104
6AA-2	832	697	601	477
6AA-1	983	808	720	553
6L	695	601	484	381
6I	1331	1142	1024	839
MAD	303	217	110	–

<sup>a</sup> Ref. 41

VDEs for all functionals, with about 60 meV errors for the SIC-SCAN and SIC-PBE. Similarly, removing self-interaction is essential for obtaining orbital energies that are consistent with electron binding. For SIC-PBE, the HOMO eigenvalues give remarkably good predictions of VDEs, with a MAE with respect to CCSD(T) of only 17 meV. An interesting feature of the FLOSIC calculations is the chemical insight that can be gained from the Fermi-orbital descriptor (FOD) positions. The FOD associated with the extra electron indicates where the the excess charge is accommodated in the clusters. In several cases, the FOD position is relatively far away from the cluster center, indicating a more delocalized density for the extra electron.

## Acknowledgement

The authors acknowledge useful discussions with Dr. Luis Basurto. This work was supported by the US Department of Energy, Office of Science, Office of Basic Energy Sciences, as part of the Computational Chemical Sciences Program under Award No. DE-SC0018331. The work of R.R.Z. was supported in part by the US Department of Energy, Office of Science, Office of Basic Energy Sciences, under Award No. DE-SC0006818. Support for computational time at the Texas Advanced Computing Center through NSF Grant No. TG-DMR090071, and at NERSC is gratefully acknowledged.

## References

- (1) Hart, E. J. In *Survey of Progress in Chemistry*; Scott, A. F., Ed.; Survey of Progress in Chemistry; Elsevier, 1969; Vol. 5; pp 129–184.
- (2) Garrett, B. C.; Dixon, D. A.; Camaioni, D. M.; Chipman, D. M.; Johnson, M. A.; Jonah, C. D.; Kimmel, G. A.; Miller, J. H.; Rescigno, T. N.; Rossky, P. J. et al. Role

- of Water in Electron-Initiated Processes and Radical Chemistry: Issues and Scientific Advances. *Chemical Reviews* **2005**, *105*, 355–390.
- (3) Kulkarni, S. A.; Bartolotti, L. J.; Pathak, R. K. Ab initio studies of anionic clusters of water pentamer. *The Journal of Chemical Physics* **2000**, *113*, 2697–2700.
- (4) Rai, D.; Kulkarni, A. D.; Gejji, S. P.; Pathak, R. K. Water Clusters (H<sub>2</sub>O)<sub>n</sub>, n=6–8, in External Electric Fields. *The Journal of Chemical Physics* **2008**, *128*, 034310.
- (5) Herbert, J. M. The quantum chemistry of loosely bound electrons. *Reviews in Computational Chemistry* **2015**, *28*, 391–517.
- (6) Herbert, J. M.; Coons, M. P. The hydrated electron. *Annual review of physical chemistry* **2017**, *68*, 447–472.
- (7) Grooß, J.-U.; Müller, R. Do cosmic-ray-driven electron-induced reactions impact stratospheric ozone depletion and global climate change? *Atmospheric Environment* **2011**, *45*, 3508–3514.
- (8) Alizadeh, E.; Orlando, T. M.; Sanche, L. Biomolecular Damage Induced by Ionizing Radiation: The Direct and Indirect Effects of Low–Energy Electrons on DNA. *Annual Review of Physical Chemistry* **2015**, *66*, 379–398.
- (9) Armbruster, M.; Haberland, H.; Schindler, H.-G. Negatively Charged Water Clusters, or the First Observation of Free Hydrated Electrons. *Phys. Rev. Lett.* **1981**, *47*, 323–326.
- (10) Hammer, N. I.; Shin, J.-W.; Headrick, J. M.; Diken, E. G.; Roscioli, J. R.; Weddle, G. H.; Johnson, M. A. How Do Small Water Clusters Bind an Excess Electron? *Science* **2004**, *306*, 675–679.
- (11) Turi, L.; Sheu, W.-S.; Rossky, P. J. Characterization of Excess Electrons in Water-Cluster Anions by Quantum Simulations. *Science* **2005**, *309*, 914–917.

- (12) Jacobson, L. D.; Herbert, J. M. Theoretical Characterization of Four Distinct Isomer Types in Hydrated-Electron Clusters, and Proposed Assignments for Photoelectron Spectra of Water Cluster Anions. *Journal of the American Chemical Society* **2011**, *133*, 19889–19899.
- (13) Rossky, P. J.; Schnitker, J. The hydrated electron: quantum simulation of structure, spectroscopy, and dynamics. *The Journal of Physical Chemistry* **1988**, *92*, 4277–4285.
- (14) Turi, L.; Rossky, P. J. Theoretical Studies of Spectroscopy and Dynamics of Hydrated Electrons. *Chemical Reviews* **2012**, *112*, 5641–5674.
- (15) Wilhelm, J.; VandeVondele, J.; Rybkin, V. V. Dynamics of the Bulk Hydrated Electron from Many-Body Wave-Function Theory. *Angewandte Chemie International Edition* **2019**, *58*, 3890–3893.
- (16) Feng, D.-F.; Kevan, L. Theoretical models for solvated electrons. *Chemical Reviews* **1980**, *80*, 1–20.
- (17) Kevan, L. Solvated electron structure in glassy matrixes. *Accounts of Chemical Research* **1981**, *14*, 138–145.
- (18) Coe, J. V.; Lee, G. H.; Eaton, J. G.; Arnold, S. T.; Sarkas, H. W.; Bowen, K. H.; Ludewigt, C.; Haberland, H.; Worsnop, D. R. Photoelectron spectroscopy of hydrated electron cluster anions,  $(\text{H}_2\text{O})_{n-}$   $n=2-69$ . *The Journal of Chemical Physics* **1990**, *92*, 3980–3982.
- (19) Kim, K. S.; Park, I.; Lee, S.; Cho, K.; Lee, J. Y.; Kim, J.; Joannopoulos, J. D. The Nature of a Wet Electron. *Phys. Rev. Lett.* **1996**, *76*, 956–959.
- (20) Kim, J.; Becker, I.; Cheshnovsky, O.; Johnson, M. A. Photoelectron spectroscopy of the ‘missing’ hydrated electron clusters  $(\text{H}_2\text{O})_{-n}$ ,  $n=3, 5, 8$  and  $9$ : Isomers and continuity

- with the dominant clusters  $n=6, 7$  and  $> 11$ . *Chemical Physics Letters* **1998**, *297*, 90 – 96.
- (21) Shin, J.-W.; Hammer, N. I.; Headrick, J. M.; Johnson, M. A. Preparation and photoelectron spectrum of the ‘missing’  $(\text{H}_2\text{O})_4^-$  cluster. *Chemical Physics Letters* **2004**, *399*, 349 – 353.
- (22) Verlet, J. R. R.; Bragg, A. E.; Kammrath, A.; Cheshnovsky, O.; Neumark, D. M. Observation of Large Water-Cluster Anions with Surface-Bound Excess Electrons. *Science* **2005**, *307*, 93–96.
- (23) Coe, J. V.; Williams, S. M.; Bowen, K. H. Photoelectron spectra of hydrated electron clusters vs. cluster size: connecting to bulk. *International Reviews in Physical Chemistry* **2008**, *27*, 27–51.
- (24) Ma, L.; Majer, K.; Chirot, F.; von Issendorff, B. Low temperature photoelectron spectra of water cluster anions. *The Journal of Chemical Physics* **2009**, *131*, 144303.
- (25) Bailey, C. G.; Kim, J.; Johnson, M. A. Infrared Spectroscopy of the Hydrated Electron Clusters  $(\text{H}_2\text{O})_n^-$ ,  $n = 6, 7$ : Evidence for Hydrogen Bonding to the Excess Electron. *The Journal of Physical Chemistry* **1996**, *100*, 16782–16785.
- (26) Ayotte, P.; Weddle, G. H.; Bailey, C. G.; Johnson, M. A.; Vila, F.; Jordan, K. D. Infrared spectroscopy of negatively charged water clusters: Evidence for a linear network. *The Journal of Chemical Physics* **1999**, *110*, 6268–6277.
- (27) Diken, E. G.; Robertson, W. H.; Johnson, M. A. The Vibrational Spectrum of the Neutral  $(\text{H}_2\text{O})_6$  Precursor to the “Magic”  $(\text{H}_2\text{O})_6^-$  Cluster Anion by Argon-Mediated, Population-Modulated Electron Attachment Spectroscopy. *The Journal of Physical Chemistry A* **2004**, *108*, 64–68.

- (28) Asmis, K. R.; Santambrogio, G.; Zhou, J.; Garand, E.; Headrick, J.; Goebbert, D.; Johnson, M. A.; Neumark, D. M. Vibrational spectroscopy of hydrated electron clusters  $(\text{H}_2\text{O})_{15-50}^-$  via infrared multiple photon dissociation. *The Journal of Chemical Physics* **2007**, *126*, 191105.
- (29) Guasco, T. L.; Elliott, B. M.; Johnson, M. A.; Ding, J.; Jordan, K. D. Isolating the Spectral Signatures of Individual Sites in Water Networks Using Vibrational Double-Resonance Spectroscopy of Cluster Isotopomers. *The Journal of Physical Chemistry Letters* **2010**, *1*, 2396–2401.
- (30) Hammer, N. I.; Roscioli, J. R.; Johnson, M. A.; Myshakin, E. M.; Jordan, K. D. Infrared Spectrum and Structural Assignment of the Water Trimer Anion. *The Journal of Physical Chemistry A* **2005**, *109*, 11526–11530.
- (31) Hammer, N. I.; Roscioli, J. R.; Johnson, M. A. Identification of Two Distinct Electron Binding Motifs in the Anionic Water Clusters: A Vibrational Spectroscopic Study of the  $(\text{H}_2\text{O})_6^-$  Isomers. *The Journal of Physical Chemistry A* **2005**, *109*, 7896–7901.
- (32) Choi, T. H.; Jordan, K. D. Potential energy landscape of the  $(\text{H}_2\text{O})_6^-$  cluster. *Chemical Physics Letters* **2009**, *475*, 293 – 297.
- (33) Lee, S.; Lee, S. J.; Lee, J. Y.; Kim, J.; Kim, K. S.; Park, I.; Cho, K.; Joannopoulos, J. Ab initio study of water hexamer anions. *Chemical Physics Letters* **1996**, *254*, 128 – 134.
- (34) Tsurusawa, T.; Iwata, S. Theoretical studies of the water-cluster anions containing the OHeHO structure: energies and harmonic frequencies. *Chemical Physics Letters* **1999**, *315*, 433 – 440.
- (35) Kim, J.; Suh, S. B.; Kim, K. S. Water dimer to pentamer with an excess electron: Ab initio study. *The Journal of Chemical Physics* **1999**, *111*, 10077–10087.

- (36) Weigend, F.; Ahlrichs, R. Abinitio treatment of (H<sub>2</sub>O)<sub>2</sub><sup>-</sup> and (H<sub>2</sub>O)<sub>6</sub><sup>-</sup>. *Phys. Chem. Chem. Phys.* **1999**, *1*, 4537–4540.
- (37) Lee, H. M.; Lee, S.; Kim, K. S. Structures, energetics, and spectra of electron-water clusters, e-(H<sub>2</sub>O)<sub>2–6</sub> and e-HOD(D<sub>2</sub>O)<sub>1–5</sub>. *The Journal of Chemical Physics* **2003**, *119*, 187–194.
- (38) Lee, H. M.; Suh, S. B.; Tarakeshwar, P.; Kim, K. S. Origin of the magic numbers of water clusters with an excess electron. *The Journal of Chemical Physics* **2005**, *122*, 044309.
- (39) Herbert, J. M.; Head-Gordon, M. Calculation of Electron Detachment Energies for Water Cluster Anions: An Appraisal of Electronic Structure Methods, with Application to (H<sub>2</sub>O)<sub>20</sub><sup>-</sup> and (H<sub>2</sub>O)<sub>24</sub><sup>-</sup>. *The Journal of Physical Chemistry A* **2005**, *109*, 5217–5229.
- (40) Herbert, J. M.; Head-Gordon, M. Accuracy and limitations of second-order many-body perturbation theory for predicting vertical detachment energies of solvated-electron clusters. *Phys. Chem. Chem. Phys.* **2006**, *8*, 68–78.
- (41) Yagi, K.; Okano, Y.; Sato, T.; Kawashima, Y.; Tsuneda, T.; Hirao, K. Water Cluster Anions Studied by the Long-Range Corrected Density Functional Theory. *The Journal of Physical Chemistry A* **2008**, *112*, 9845–9853.
- (42) Ünal, A.; Bozkaya, U. Anionic water pentamer and hexamer clusters: An extensive study of structures and energetics. *The Journal of Chemical Physics* **2018**, *148*, 124307.
- (43) Zho, C.-C.; Vlček, V.; Neuhauser, D.; Schwartz, B. J. Thermal Equilibration Controls H-Bonding and the Vertical Detachment Energy of Water Cluster Anions. *The Journal of Physical Chemistry Letters* **2018**, *9*, 5173–5178.
- (44) Becke, A. D. A new mixing of Hartree-Fock and local density functional theories. *The Journal of Chemical Physics* **1993**, *98*, 1372–1377.

- (45) Sun, J.; Ruzsinszky, A.; Perdew, J. P. Strongly Constrained and Appropriately Normed Semilocal Density Functional. *Phys. Rev. Lett.* **2015**, *115*, 036402.
- (46) Chen, M.; Ko, H.-Y.; Remsing, R. C.; Andrade, M. F. C.; Santra, B.; Sun, Z.; Selloni, A.; Car, R.; Klein, M. L.; Perdew, J. P. et al. Ab initio theory and modeling of water. *Proceedings of the National Academy of Sciences* **2017**, *114*, 10846–10851.
- (47) Perdew, J. P.; Burke, K.; Ernzerhof, M. Generalized Gradient Approximation Made Simple. *Phys. Rev. Lett.* **1996**, *77*, 3865–3868.
- (48) Perdew, J. P.; Zunger, A. Self-interaction correction to density-functional approximations for many-electron systems. *Phys. Rev. B* **1981**, *23*, 5048–5079.
- (49) Pederson, M. R.; Heaton, R. A.; Lin, C. C. Local-density Hartree-Fock theory of electronic states of molecules with self-interaction correction. *The Journal of Chemical Physics* **1984**, *80*, 1972–1975.
- (50) Pederson, M. R.; Heaton, R. A.; Lin, C. C. Density functional theory with self-interaction correction: Application to the lithium molecules). *The Journal of Chemical Physics* **1985**, *82*, 2688–2699.
- (51) Pederson, M. R.; Ruzsinszky, A.; Perdew, J. P. Communication: Self-interaction correction with unitary invariance in density functional theory. *The Journal of Chemical Physics* **2014**, *140*, 121103.
- (52) Löwdin, P. On the Non-Orthogonality Problem Connected with the Use of Atomic Wave Functions in the Theory of Molecules and Crystals. *The Journal of Chemical Physics* **1950**, *18*, 365–375.
- (53) Pederson, M. R. Fermi orbital derivatives in self-interaction corrected density functional theory: Applications to closed shell atoms. *The Journal of Chemical Physics* **2015**, *142*, 064112.

- (54) Pederson, M. R.; Baruah, T. In *Chapter Eight - Self-Interaction Corrections Within the Fermi-Orbital-Based Formalism*; Arimondo, E., Lin, C. C., Yelin, S. F., Eds.; Advances In Atomic, Molecular, and Optical Physics; Academic Press, 2015; Vol. 64; pp 153 – 180.
- (55) Liu, D. C.; Nocedal, J. On the limited memory BFGS method for large scale optimization. *Mathematical programming* **1989**, *45*, 503–528.
- (56) Yamamoto, Y.; Diaz, C. M.; Basurto, L.; Jackson, K. A.; Baruah, T.; Zope, R. R. Fermi-Löwdin orbital self-interaction correction using the strongly constrained and appropriately normed meta-GGA functional. *The Journal of Chemical Physics* **2019**, *151*, 154105.
- (57) Baruah, T.; Yamamoto, Y.; Basurto, L.; Diaz, C. M.; Zope, R. R. Self-interaction correction to density functional approximations using Fermi-Löwdin orbitals: Methodology and Parallelization. (unpublished).
- (58) Jackson, K.; Pederson, M. R. Accurate forces in a local-orbital approach to the local-density approximation. *Phys. Rev. B* **1990**, *42*, 3276–3281.
- (59) Pederson, M.; Porezag, D.; Kortus, J.; Patton, D. Strategies for Massively Parallel Local-Orbital-Based Electronic Structure Methods. *physica status solidi (b)* **2000**, *217*, 197–218.
- (60) Porezag, D.; Pederson, M. R. Optimization of Gaussian basis sets for density-functional calculations. *Phys. Rev. A* **1999**, *60*, 2840–2847.
- (61) Pederson, M. R.; Jackson, K. A. Variational mesh for quantum-mechanical simulations. *Phys. Rev. B* **1990**, *41*, 7453–7461.
- (62) Kao, D.-y.; Withanage, K.; Hahn, T.; Batool, J.; Kortus, J.; Jackson, K. Self-consistent self-interaction corrected density functional theory calculations for atoms using Fermi-

- Löwdin orbitals: Optimized Fermi-orbital descriptors for Li–Kr. *The Journal of Chemical Physics* **2017**, *147*, 164107.
- (63) Withanage, K. P.; Trepte, K.; Peralta, J. E.; Baruah, T.; Zope, R.; Jackson, K. A. On the Question of the Total Energy in the Fermi–Löwdin Orbital Self-Interaction Correction Method. *Journal of chemical theory and computation* **2018**, *14*, 4122–4128.
- (64) Pederson, M. R.; Baruah, T.; Kao, D.-y.; Basurto, L. Self-interaction corrections applied to Mg-porphyrin, C<sub>60</sub>, and pentacene molecules. *The Journal of Chemical Physics* **2016**, *144*, 164117.
- (65) Sharkas, K.; Li, L.; Trepte, K.; Withanage, K. P.; Joshi, R. P.; Zope, R. R.; Baruah, T.; Johnson, J. K.; Jackson, K. A.; Peralta, J. E. Shrinking Self-Interaction Errors with the Fermi–Löwdin Orbital Self Interaction Corrected Density Functional Approximation. *The Journal of Physical Chemistry A* **2018**, *122*, 9307–9315.
- (66) Shahi, C.; Bhattarai, P.; Wagle, K.; Santra, B.; Schwalbe, S.; Hahn, T.; Kortus, J.; Jackson, K. A.; Peralta, J. E.; Trepte, K. et al. Stretched or noded orbital densities and self-interaction correction in density functional theory. *The Journal of Chemical Physics* **2019**, *150*, 174102.
- (67) Kao, D.-y.; Pederson, M.; Hahn, T.; Baruah, T.; Liebing, S.; Kortus, J. The Role of Self-Interaction Corrections, Vibrations, and Spin-Orbit in Determining the Ground Spin State in a Simple Heme. *Magnetochemistry* **2017**, *3*, 31.
- (68) Joshi, R. P.; Trepte, K.; Withanage, K. P.; Sharkas, K.; Yamamoto, Y.; Basurto, L.; Zope, R. R.; Baruah, T.; Jackson, K. A.; Peralta, J. E. Fermi–Löwdin orbital self-interaction correction to magnetic exchange couplings. *The Journal of Chemical Physics* **2018**, *149*, 164101.
- (69) Johnson, A. I.; Withanage, K. P.; Sharkas, K.; Yamamoto, Y.; Baruah, T.; Zope, R. R.; Peralta, J. E.; Jackson, K. A. The effect of self-interaction error on electrostatic dipoles

- calculated using density functional theory. *The Journal of Chemical Physics* **2019**, *151*, 174106.
- (70) Withanage, K. P.; Akter, S.; Shahi, C.; Joshi, R. P.; Diaz, C.; Yamamoto, Y.; Zope, R.; Baruah, T.; Perdew, J. P.; Peralta, J. E. et al. Self-interaction-free electric dipole polarizabilities for atoms and their ions using the Fermi-Löwdin self-interaction correction. *Physical Review A* **2019**, *100*, 012505.
- (71) Perdew, J. P.; Parr, R. G.; Levy, M.; Balduz Jr, J. L. Density-functional theory for fractional particle number: derivative discontinuities of the energy. *Physical Review Letters* **1982**, *49*, 1691.
- (72) Levy, M.; Perdew, J. P.; Sahni, V. Exact differential equation for the density and ionization energy of a many-particle system. *Physical Review A* **1984**, *30*, 2745.
- (73) Perdew, J. P.; Levy, M. Comment on “Significance of the highest occupied Kohn-Sham eigenvalue”. *Physical Review B* **1997**, *56*, 16021.
- (74) Harbola, M. K. Relationship between the highest occupied Kohn-Sham orbital eigenvalue and ionization energy. *Phys. Rev. B* **1999**, *60*, 4545–4550.
- (75) Odutola, J. A.; Dyke, T. R. Partially deuterated water dimers: Microwave spectra and structure. *The Journal of Chemical Physics* **1980**, *72*, 5062–5070.
- (76) Sharkas, K.; Wagle, K.; Santra, B.; Akter, S.; Zope, R. R.; Baruah, T.; Jackson, K.; Perdew, J. P.; Peralta, J. preprint.
- (77) Perdew, J. P.; Schmidt, K. Jacob’s ladder of density functional approximations for the exchange-correlation energy. AIP Conference Proceedings. 2001; pp 1–20.
- (78) Becke, A. D. Density functional exchange energy approximation with correct asymptotic behavior. *Phys. Rev. A* **1988**, *38*, 3098–3100.

- (79) Lee, C.; Yang, W.; Parr, R. G. Development of the Colle-Salvetti correlation-energy formula into a functional of the electron density. *Phys. Rev. B* **1988**, *37*, 785–789.
- (80) Tsuneda, T.; Suzumura, T.; Hirao, K. A reexamination of exchange energy functionals. *The Journal of Chemical Physics* **1999**, *111*, 5656–5667.
- (81) Verma, P.; Perera, A.; Bartlett, R. J. Increasing the applicability of DFT I: Non-variational correlation corrections from Hartree–Fock DFT for predicting transition states. *Chemical Physics Letters* **2012**, *524*, 10–15.
- (82) Kim, M.-C.; Sim, E.; Burke, K. Understanding and reducing errors in density functional calculations. *Phys. Rev. Lett.* **2013**, *111*, 073003.